Offprinted from the *Journal of The Chemical Society, Faraday Transactions II*, 1975, vol. 71.

Far Infra-red Manifestations of the Intermolecular Dynamics in Compressed Gaseous and Liquid $CClF_3$

By Graham J. Davies

Post Office Research Department, Dollis Hill, London NW2 7DT

and

Myron Evans*

Edward Davies Chemical Laboratories, University College of Wales, Aberystwyth SY23 1NE

Received 14*th July*, 1974

The spectra of chlorotrifluoromethane ($CClF_3$) have been taken in the region 2–100 cm^{-1} at pressures of 1.0–147.7 bar, and in the liquid phase. In all cases, the pure rotational envelope is dominant, suggesting that, even in the liquid, the molecular dynamics are those of collision-interrupted almost-free rotation. Mean times between collisions have been estimated by comparing vectorial correlation functions derived from the experimental data with those predicted by McClung's extended *J*-diffusion model. The higher frequency parts of the bands observed have their origin in collision-induced dipolar absorption, which has been quantitatively treated using equations for multipole-induced dipolar absorption in bimolecular collisions derived from Frost's general theory for symmetric top molecules. Using these equations, an approximate value for the quadrupole moment ($|Q|$) of 11×10^{-40} C m^2 has been estimated from moderately low pressure data. The value of $|Q| \doteqdot 6 \times 10^{-40}$ C m^2 obtained in the same way from the liquid and highly compressed gaseous data reflects *inter alia* the loss of validity of the bimolecular collision model and of the point multipole expansion of the molecular field when the mean distance travelled between collisions is of the order of the molecular van der Waals diameter. This last point is illustrated using a local charge basis for the field in the near neighbourhood of a molecule.

This work aims to study the contribution of collision-induced dipolar absorption to the observed far infra-red spectrum (3–100 cm^{-1}) of the symmetric top molecule $CClF_3$ in the compressed gaseous and liquid states. One way of elucidating molecular rotations, hindered or otherwise, in the fluid is to observe the effect on the pure rotational envelope of increasing the molecular number density so that two body and higher order collisions become statistically significant. The envelope then acquires a high frequency tail, which is the spectral consequence of a collision-induced dipolar absorption, in addition to that of the permanent dipole. This tail is the result in the frequency domain of significant collisional damping of the free rotational motion in the time domain.

The induced dipole can be evaluated using Frost's theory [1] by expanding the field of the one molecule at a second in terms of its point multipoles assuming the following. (1) An eigenstate of the interacting pair is taken as the product of the eigenstates of the isolated molecules. This is adequate only for a purely central intermolecular potential $U(R)$, which can then be approximated by a Lennard-Jones potential. (2) The centre of mass motion of each molecule in a pairwise interaction is treated classically, with each molecule at rest, so translational absorption is ignored.

* present address: Physical Chemistry Laboratory, South Parks Road, Oxford OX1 3QZ.

It is possible to determine an apparent quadrupole moment for the species involved if the induced dipolar absorption intensity is measured experimentally. For this particular molecule, the order of magnitude contribution of octopole-induced dipolar absorption can be estimated, using a literature [2] value for Ω, the octopole moment.

When the molecular number density reaches that value at which the proportion of three or more body collisions is significant the bimolecular collision model becomes a poor approximation, a circumstance reflected in the apparent drift in the quadrupole moment estimates.

This particular molecule is chosen because:

(*a*) its pseudo-spherical geometry is such that a Lennard-Jones form for $U(R)$ is a fair approximation;

(*b*) a low dipole moment means that the permanent dipolar contribution will not be overwhelming [3];

(*c*) its critical properties are such that the gas can be conveniently compressed to liquid-like densities;

(*d*) of its chemical inertness.

EXPERIMENTAL

The spectra have been obtained by Fourier spectrometry [4-6] with two interferometers. The region 20–100 cm^{-1} was covered with a resolution of 4 cm^{-1} using amplitude modulation of the radiation reaching a Golay SP16 pneumatic detector. A commercially available interferometer was modified to cover the spectral range 2 to 31 cm^{-1}. The air-cooled lamp-housing was replaced by a more efficient water-cooled unit and phase modulation was incorporated.[6, 7] During the period when the experimental observations were being made the apparatus was left permanently switched on to ensure maximum stability. These measures improved the quality of the results.

For the range 2–31 cm^{-1} a Rollin-InSb, liquid helium-cooled detector [8] was employed together with a 4 mm black-polyethylene filter. Signal-to-noise ratios as great as 10 000 were obtained, while the reproducibility of three consecutive runs was estimated to be of the order of 0.1 %. The resolution was usually 2 cm^{-1}, and 0.5 cm^{-1} for the data at 1 bar.

Three sample cells of different path lengths were used. The high pressure and liquid spectra were taken in a variable path length, high pressure cell [3] with 7 mm Z-cut crystalline quartz windows. To avoid spurious effects arising from refractive index differences, these spectra were obtained by taking the ratio of the mean of several long path length interferograms to that of the corresponding short path length ones.

The data at 4.4 bar, 288 K were collected using a 137.6 mm high pressure gas cell designed and built by Mr. Harold Jolley at the Edward Davies Chemical Laboratories, Aberystwyth. This cell fits the " module H " of the N.P.L./Grubb-Parsons cube interferometer and is itself of modular construction so that different path lengths may be employed. It consists of a 12 mm o.d. gold-plated copper light pipe embedded in a stainless steel surround, with a similar light cone leading to the detector. Variable thicknesses of quartz, TPX, or polypropylene windows may be employed as the spectral, pressure, and energy-throughput characteristics demand. Thermocouple posts are drilled at intervals in the stainless steel body to within a millimetre or so of the working surface. This section is linked to a stainless steel sample drying chamber containing pre-baked type-3A zeolite.[3]

The spectrum at 1 bar, 288 K was taken with a 0.5 cm^{-1} resolution using a 260 mm length of glass tubing attached to the " H-module ". No attempt was made to remove traces of water vapour, because of the relatively weak absorption of the latter in this region.

The nominal purity of the commercial sample (Matheson) of gas used was 99 % w/w min., having the following specified [10] impurities: moisture 10 p.p.m. w/w; high boilers 0.05 % (by vol.); air (vap.) 1.0 % (by vol.); acidity nil. The moisture content of the gas sample was kept low by several freeze-pump-thaw cycles wherein the gas was frozen onto the zeolite using a solid CO_2 or $N_2(l)$ slush bath, any volatiles remaining being pumped off to about 10^{-2} Torr.

The noise scatter of the Golay detector between individual runs is the cause of a $\pm(2\text{-}5)\%$ uncertainty in $A_1 = \int_{\text{band}} \alpha(\bar{\nu})\, d\bar{\nu}$. Contributions to the uncertainty in the estimated molecular number density (N) are listed.

(i) The necessity of heating the cell to well above the critical temperature (301.9 K) in the runs where the critical pressure (38.2 bar) was exceeded. This results in a slight temperature gradient between the front and back windows. The mean measured temperature has uncertainty limits of about ± 1.5 % on the Kelvin scale.

(ii) The pressure, as monitored by a Budenberg gauge, was constant to about ± 0.3 bar once equilibrium of the cell heating systems was obtained (*ca.* 4 h).

These factors results in a total estimated uncertainty in N of about ± 3.5 %.

The liquid density was estimated using the molar refraction equation via accurate refractive index data.[11]

RESULTS

The spectra of the compressed gas, from 1.0–147.7 bar, are illustrated in fig. 1 to 3, together with that of the liquid at 288 K. Immediate observations are summarised in table 1.

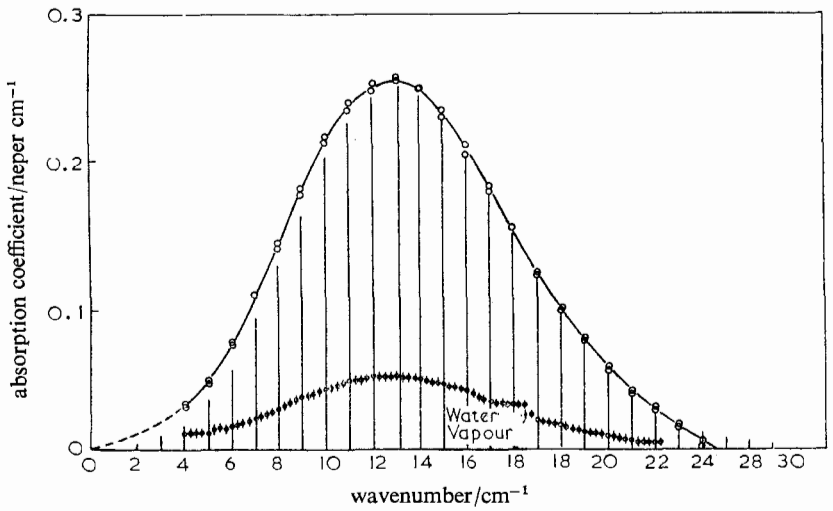

FIG. 1.—Power absorption coefficient of $CClF_3$ at low pressures. ϕ = 1 atm, 288 K; 0 = 4.4 atm, 288 K. The vertical lines give the frequencies and relative integrated intensities of some of the pure rotational ($J \rightarrow J+1$) transitions up to $J = 150$.

TABLE 1.—PRESSURE DEPENDENCE OF THE FAR INFRA-RED ABSORPTION IN $CClF_3$

pressure/bar	temp./K	exptl.[12] compressibility	$10^{-21}\,N/\text{cm}^{-3}$	$\bar{\nu}_{max}/\text{cm}^{-1}$	α_{max}/neper cm^{-1}	A_1/neper cm^{-2}
1.0(0)	288	0.98	0.02(6)	12.5	0.05	0.59
4.4(2)	288	0.96	0.11(7)	12.9	0.26	3.01
40.4	323	0.63	1.46	13.3	2.53	53.(7)
67.7	323	0.34(5)	4.46	13.3	6.23	162.(3)
104.3	323	0.43	5.51	13.3	6.97	186.(0)
147.7	323	0.56	5.99	13.3	7.40	212.(4)
liquid	288	—	5.28	13.0	7.60	222.(6)

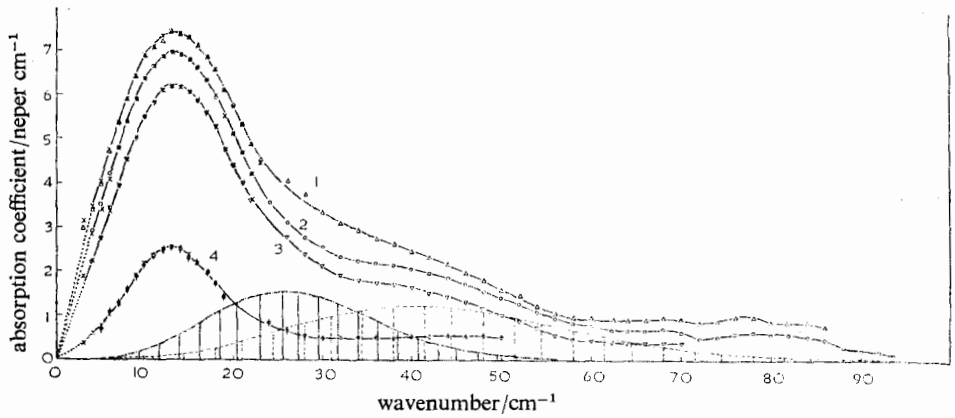

FIG. 2.—Power absorption coefficient of $CClF_3$ at high pressures. Curve 4, 40.4 bar and 323 K; curve 3, 67.7 bar and 323 K; curve 2, 104.3 bar and 323 K; curve 1, 147.7 bar and 323 K. The vertical solid lines give the frequencies and relative integrated intensities of some of the quadrupole-induced ($J \rightarrow J+2$) transitions. The vertical dashed lines give the frequencies and relative integrated intensities of some of the octopole-induced ($J \rightarrow J+3$) transitions.

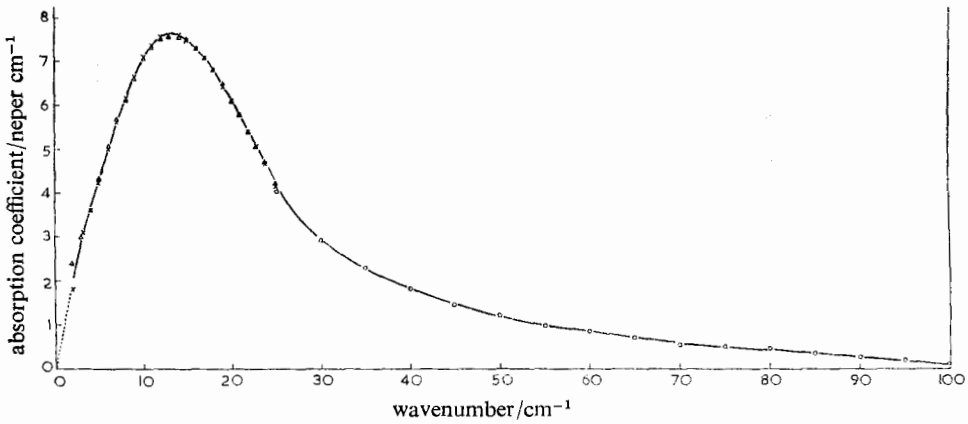

FIG. 3.—Power absorption coefficient of liquid $CClF_3$ at 288 K.

The bar spectra in fig. 2 show the frequencies and relative integrated intensities of some of the quadrupole induced ($J \rightarrow J+2$) and octopole-induced ($J \rightarrow J+3$) transitions at 323 K.

EVALUATION AND DISCUSSION OF RESULTS

As the aim is to extract information on the molecular interactions and dynamics it is appropriate to describe the response of the gas/liquid system to an external electromagnetic perturbation in terms of the transition dipole moment and related features. The response of the system, measured as an absorption coefficient is directly related by Fourier transformation to the change of the statistical average of the transition dipole moment with time, so that, according to Gordon [14] the complex dipole correlation function $C^*(t)$ is given by:

$$C^*(t) = \langle \boldsymbol{P}(0) \cdot \boldsymbol{P}(t) \rangle = \int_{-\infty}^{\infty} I(\bar{\nu}) \exp(2\pi i \bar{\nu} c t)\, \mathrm{d}\bar{\nu} \qquad (1)$$

where

$$I(\bar{\nu}) = \frac{3hn(\bar{\nu})\alpha(\bar{\nu})}{16\pi^4(1-\exp(-h\bar{\nu}c/kT))\bar{\nu}}. \quad (2)$$

Here, P is in general a first order Legendre polynomial, $n(\bar{\nu})$ is the frequency dependent refractive index, $\alpha(\bar{\nu})$ the absorption coefficient, $\bar{\nu}$ the frequency in wavenumbers.

An expression for the real part of $C^*(t)$, taking account of the " dynamic " Onsager internal field, has been obtained recently by Gerschel *et al.*[15] (their eqn (11)) and this has been used to compute normalised dipole correlation functions from our $(\alpha(\bar{\nu}), \bar{\nu})$ data (see fig. 5).

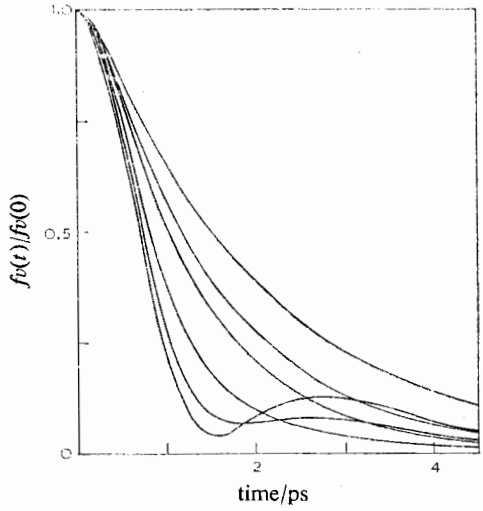

FIG. 4.—Theoretical [16] vectorial correlation functions for $CClF_3$ at 288 K. From top to bottom, the curves are for values of τ_J, the mean time between collisions, of: 0.2 ps, 0.3 ps, 0.4 ps, 0.9 ps, 3.0 ps and $\tau_J \rightarrow \infty$ (free rotor), respectively.

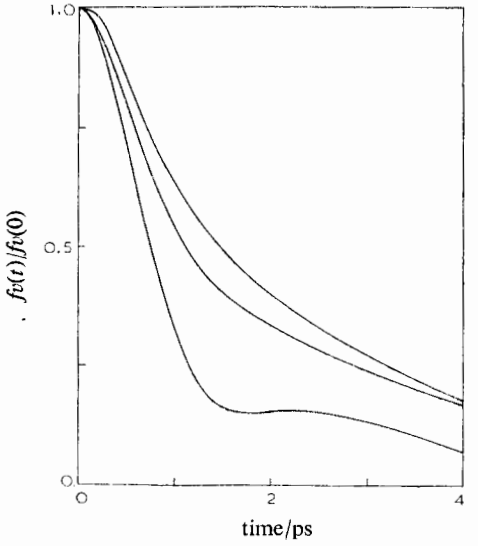

FIG. 5.—Some representative, experimental vectorial correlation functions for $CClF_3$. From top to bottom: liquid; gas at 67.7 bar and 320 K; gas at 40.4 bar and 320 K.

The experimental data are now in a form more suitable for direct comparison with theoretical vectorial correlation functions computed from specific models of the intermolecular dynamics such as the extended J-diffusion model of McClung [16] for the collision-interrupted free rotation of symmetric top molecules. In the J-diffusion model [17] the angular momentum of a rotator is randomised in both magnitude and direction at every collision. No assumptions are made about the average duration of a period of free rotation, whereas the diffusion equation is valid only if the average duration of a period of free rotation is much shorter than the average time for complete rotation of the molecule. Each period of free rotation is microscopically studied in the extended diffusion model; inertial effects are therefore accounted for. Eagles and McClung [18] have developed an efficient method of computing free rotor memory functions and J-diffusion reorientational correlation functions from the associated memory functions. From a comparison (fig. 4) of the theoretical and experimental functions, it is possible to estimate for each set of experimental data a mean time between collisions (τ_J) and thence the mean distance travelled by a molecule between successive collisions, from kinetic theory. The J-diffusion model has been compared with the experimental function at three representative number densities, giving mean free paths between collisions from kinetic theory as listed:

N/molecule $cm^{-3} = 5.28 \times 10^{21}$; 4.46×10^{21}; 1.46×10^{21}
mean free path/nm = 0.1 (1.0 Å); 0.15 (1.5 Å); ~1.8 nm (18 Å).

The shorter mean free path in the liquid may be indicative of the greater probability of triple and higher order collisions in the condensed phase, whereas in the more dilute gas phase it is valid to use a model of almost exclusively bimolecular encounters.

It is interesting to note that the position of $\bar{\nu}_{max}$ does not change significantly between the dilute gas and the liquid, this being in contrast to a shift of 25 cm^{-1} in CO_2,[19] 30 cm^{-1} in N_2O,[3] and 60 cm^{-1} in propyne [20] and in accord with a correspondingly small shift [3] for fluoroform. One conclusion that can be drawn immediately from the present results is that the absorption process in the liquid is still dominated by almost free rotation of the molecule. The barrier to rotation is small, the combination of molecular isotropy and low liquid density being indicative of a process of collision-interrupted molecular free rotation rather than collision-interrupted libration.[21] To test this hypothesis further, the short-time motion has been examined using the rotational velocity correlation function [15] defined as the negative of the second derivative of the real part of $C^*(t)$. Gerschel's [15] eqn (13) has been used to obtain these functions from the experimental ($\alpha(\bar{\nu})$, $\bar{\nu}$) data; they are illustrated in fig. 7 and 8. It is necessary to obtain the corresponding function for the free rotation of a symmetric top molecule rather precisely in order that the extent of collisional damping may be estimated by comparison.

In the free rotation of symmetric top molecules, the discrete expression for the integrated intensity of the $J \rightarrow J+1$ ($\Delta K = 0$) allowed transition is [20]:

$$\bar{A}(J \rightarrow J+1) = A(I, J) \sum_{K=-J}^{J} S(I, K) \frac{(J+1)^2 - K^2}{(J+1)} \exp(-E(J, K)hc/kT) \qquad (3)$$

where*

$$A(I, J) = \frac{8\pi^3 N}{3hcZ} \mu^2 \bar{\nu}(J)(1 - \exp(-hc\bar{\nu}(J)/kT))$$

$$S(I, K) = \tfrac{1}{3}(2I+1)(4I^2+4I+3) \text{ for } K = 0,$$
$$= \tfrac{1}{3}(2I+1)(4I^2+4I+3) \text{ for } K \neq 0,\ K = \text{multiple of 3},$$
$$= \tfrac{1}{3}(2I+1)(4I^2+4I) \text{ for } K \neq 0,\ K \neq \text{multiple of 3};$$

* unrationalised units.

$$E(J, K) = BJ(J+1)+(A-B)K^2;$$

$$Z = \sum_{J} \sum_{K=-J}^{J} g(J, K)\exp(-E(J, K)/kT);$$

$$g(J, K) = (2J+1)S(I, K);$$

I = nuclear spin quantum number of the off axis nuclei.

From eqn 1, 2 and 3

$$I(\bar{\nu}) \propto \sum_{K=-J}^{J} S(I, K)\frac{(J+1)^2-K^2}{(J+1)} \exp(-E(J, K)\boldsymbol{hc}/\boldsymbol{kT}).$$

Defining $C^*(t)$ by

$$C^*(t) = R(t)+\mathrm{i}\, I(t) \tag{4}$$

we have the rotational velocity correlation function $R_f''(t)$ as:

$$R_f''(t) = -\frac{\mathrm{d}^2}{\mathrm{d}t^2}(R(t)) \tag{5}$$

with

$$R(t) = 2\int_0^{\infty} I(\bar{\nu}) \cos 2\pi\bar{\nu}ct \,\mathrm{d}\bar{\nu}. \tag{6}$$

Using (4), (5) and (6) one finds that:

$$R_f''(t) \propto \int_0^{\infty} \sum_{K=-J}^{J}\left[S(I, K)\left(\frac{\bar{\nu}^3}{2B}-2B\bar{\nu}K^2\right)\exp\left(\frac{-(|A-B|)K^2\boldsymbol{hc}}{\boldsymbol{kT}}\right)\right]\times \exp\left(-\frac{B\boldsymbol{hc}}{\boldsymbol{kT}}\left(\frac{\bar{\nu}}{2B}-1\right)\cdot\frac{\bar{\nu}}{2B}\right)\cos(2\pi\bar{\nu}ct)\,\mathrm{d}\bar{\nu} \tag{7}$$

where J in (7) is given by the *integer* $(\bar{\nu}/2B-1)$.

Thus we arrive at the " semi-discrete " expression (7) which is that for the rotational velocity correlation function of a Boltzmann weighted system of symmetric

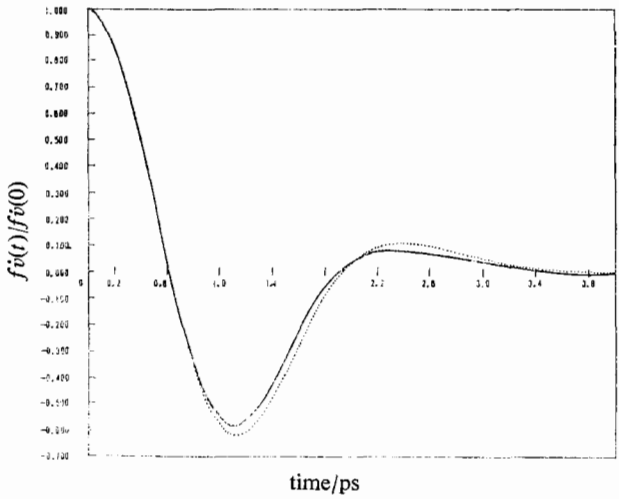

FIG. 6.—Rotational velocity correlation functions for $CClF_3$. —— experimental at 4.4 bar an 288 K; . . . . . theoretical using the free rotor expression eqn (7).

top molecules. This equation has been evaluated using numerical integration by Simpson's rule with integration intervals of $2B$. (In this way it is ensured that the summation over K is made with the correct values of J given by $\bar{\nu}/2B-1$. Because of the exponential weighting, the limits 0 to $2B$ $(4x+1)$ where x is a positive integer have been found to give stable values of $R_f''(t)$.)

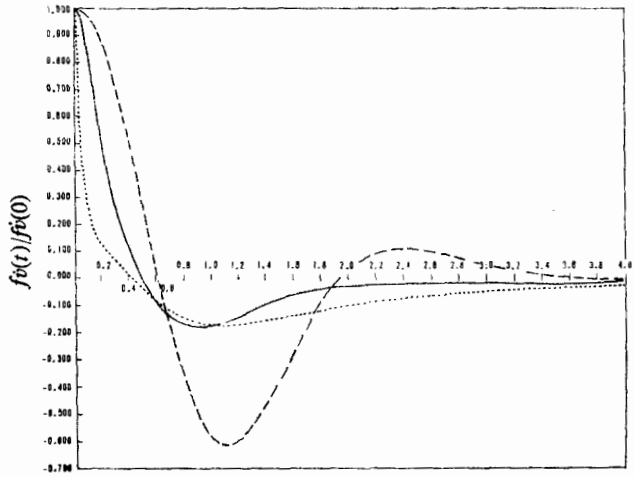

FIG. 7.—Rotational velocity correlation function for $CClF_3$. —— liquid at 288 K; - - - - - free rotor model; . . . . . Brot model with $\tau_r = 1.5$ ps, $\tau = 0.15$ ps and $\tau_a = 0.25$ ps.

The rotational velocity correlation function calculated from the experimental data at 4.4 bar, 288 K, is shown in fig. 6 together with this free rotor function. Whereas the overall profiles are very similar, the experimental data, which are accurate to within ± 0.5 %, show slight collisional damping. The higher density data yield rota-

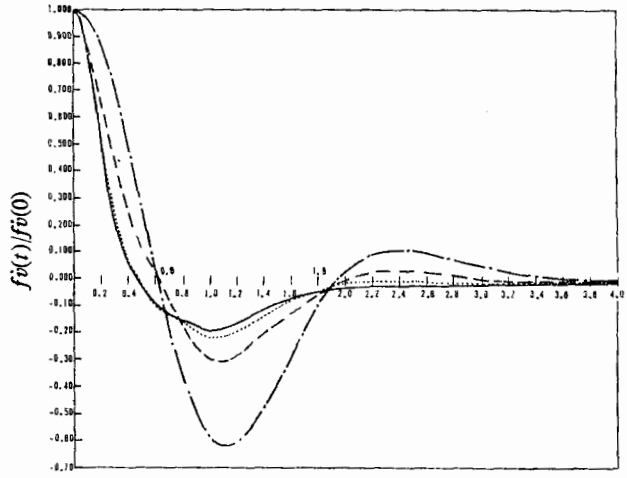

FIG. 8.—Experimental rotational velocity correlation functions for $CClF_3$. —— gas at 147.7 bar and 313 K; . . . . . gas at 67.7 bar and 313 K; - - - - gas at 40.4 ± 0.5 bar and 313 K; - . - . - . - theoretical free rotor expression.

tional velocity correlation functions (fig. 8) which show considerable damping. The curve derived from the liquid data has been compared (fig. 7) with a corresponding theoretical expression derived from a model of collision perturbed librators [21, 22] using a mean time between collisions of 0.5 ps, with a mean time of residence within a given librational well [21] of 1.5 ps. The rather poor line-shape agreement obtained seems to be further evidence of quasi-free collision interrupted rotation of the $CClF_3$ (1) just above the critical pressure, rather than libration.

MULTIPOLE ANALYSIS

The data can be treated in terms of multipolar induced dipole absorption using the following equation:

$$A_1 = \int_{\text{band}} \alpha(\bar{\nu})\, \mathrm{d}\bar{\nu} = AN + (A^{\mu} + A^{Q} + A^{\Omega})N^2. \tag{8}$$

Eqn (8) implies that triple and higher order collisions are completely neglected in our analysis. The integrated absorption intensity A_1 is assumed to arise from a pure rotational contribution of the permanent dipole proportional to N; and from an induced component $(A^{\mu}+A^{Q}+A^{\Omega})N^2$ arising from bimolecular collisions. The proportionality constant A can be calculated by summing (3) over positive integral J, which yields a value of $A/N = 2.317\times10^{-20}$ cm at 288 K, and 2.316×10^{-20} cm at 330 K. Alternatively, A/N, is given by the sum rule of Gordon [23] as:

$$\frac{A}{N} = \frac{2\pi\mu_z^2}{3c^2 I_x} = 2.32\times10^{-20}\ \text{cm},$$

where I_x is the moment of inertia about either axis perpendicular to the one containing the permanent dipole μ_z. Thus A/N is well defined.

The constant $(A^{\mu}+A^{Q}+A^{\Omega})$ is composed of the terms A^{μ}, A^{Q} and A^{Ω} which represent the absorption intensity of the dipole induced in one molecule by the dipole, quadrupole, and octopole fields, respectively, of the other in a bimolecular collision. The multipole expansion of the molecular electrostatic potential has been terminated at the octopole in eqn (8), so that hexadecapole and higher multipoles are neglected.

The general theory of pressure-induced absorption by symmetric top molecules has been given recently by Frost.[1] The basic equation* for the intensity (I_{AA}) of the bimolecular collision induced dipolar absorption is as follows:

$$I_{AA} = \frac{4\pi^3\bar{\nu}N^2}{3hc} \sum_{\substack{i,f \\ (E_f - E_i \approx h\nu)}} \left(\frac{F_i^{AA}}{d_i^{AA}} - \frac{F_f^{AA}}{d_f^{AA}}\right) \int_0^{\infty} 4\pi R^2 \exp(-U_{AA}(R)/kT) \times \sum_{m_i, m_f} |\langle im_i|\mu^{AA}(R)|fm_f\rangle|^2\, \mathrm{d}R \tag{9}$$

where $\boldsymbol{\mu}(R)$ is the *induced* dipole moment of a pair of molecules separated by R, and where $|im_i\rangle$, $|fm_f\rangle$ denote in general rotation-vibration eigenstates for the pair, with m_i, m_f as degenerate magnetic quantum numbers. The summations over the quantum numbers i, f are restricted to those transitions $i \rightarrow f$ for which the absorbed frequency $h^{-1}(E_f - E_i)$ lies in the absorption band of (approximate) frequency ν. The quantities d_i, d_f are the degeneracies of the quantum numbers i, f respectively. $U_{AA}(R)$ is the intermolecular potential energy. F_i is given by the Maxwell–Boltzmann expression:

$$F_i = d_i \exp(-E_i/kT)/Z \tag{10}$$

* unrationalised units.

where the partition function

$$Z = \sum_i d_i \exp(-E_i/kT). \tag{11}$$

The summation is carried out over all allowed energy levels and it can be shown that [3, 5]:

$$\sum_{\substack{i,f \\ (E_f - E_i \approx h\nu)}} \left(\frac{F_i^{AA}}{d_i^{AA}} - \frac{F_f^{AA}}{d_f^{AA}}\right) = \frac{1}{Z}\exp(-E_i/kT)(1-\exp(-hc\bar{\nu}_{if}/kT))S(I, K). \tag{12}$$

The matrix elements $\Sigma|\langle im_i|\mu^{AA}(R)|fm_f\rangle|^2$ are expanded by Frost (his eqn (24)) as:

$$\sum_{\lambda_1,\lambda_2}\left[(\sum|Fm|^2)\frac{(2J_1+1)}{(2\lambda_1+1)}C(J_1, \lambda_1, J_1'; K_1, K_1'-K_1, K_1')^2 \times \frac{(2J_2+1)}{(2\lambda_2+1)}C(J_2, \lambda_2, J_2'; K_2, K_2'-K_2, K_2')^2\right] \tag{13}$$

where $\Sigma|Fm|^2$ is listed in table 2 for various λ_1 and λ_2. The C coefficients are the relevant Clebsch–Gordan factors.

TABLE 2.—THE ELEMENTS $\Sigma|Fm|^2$ OF EQN (13) FOR VARIOUS λ_i

λ_1	λ_2	$\Sigma\|Fm\|^2$
0	1	$6\alpha_0^2\mu^2R^{-6}$
0	2	$15\alpha_0^2Q^2R^{-8}$
2	1	$20/3(\delta^2\mu^2R^{-6})$
2	2	$40/3(\delta^2Q^2R^{-8})$
0	3	$(\lambda_2+1)(2\lambda_2+1)\alpha_0^2\Omega^2R^{-10}$
2	3	$10/9(\lambda_2+1)(2\lambda_2+1)\delta^2\Omega^2R^{-10}$

In table 2, Q is the quadrupole moment, $\alpha_0 = \frac{1}{3}(2\alpha_\perp+\alpha_\parallel)$ is the mean molecular polarisability, $\delta = (\alpha_\parallel - \alpha_\perp)$ is the anistropy of polarisability, and μ is the *permanent* dipole moment.

TABLE 3.—ALLOWED TRANSITIONS UP TO THE OCTOPOLE MOMENT TERM IN SYMMETRIC TOPS (✓)

				(λ_1, λ_2)										
ΔJ_1	ΔJ_2	ΔK_1	ΔK_2	(0, 3)	(0, 2)	(0, 1)	(1, 2)	(1, 0)	(2, 3)	(2, 2)	(2, 1)	(2, 0)	(3, 2)	(3, 0)
0	1	0	0	✓	✓	✓	✓	×	✓	✓	✓	×	✓	×
0	2	0	0	✓	✓	×	✓	×	✓	✓	×	×	✓	×
1	0	0	0	×	×	×	✓	✓	✓	✓	✓	✓	✓	✓
1	1	0	0	×	×	×	✓	×	✓	✓	✓	×	✓	×
1	2	0	0	×	×	×	✓	×	✓	✓	×	×	✓	×
2	0	0	0	×	×	×	×	×	✓	✓	✓	✓	✓	✓
2	1	0	0	×	×	×	×	×	✓	✓	✓	×	✓	×
2	2	0	0	×	×	×	×	×	✓	✓	×	×	✓	×
3	0	0	0	×	×	×	×	×	×	×	×	×	✓	✓
3	1	0	0	×	×	×	×	×	×	×	×	×	✓	×
3	2	0	0	×	×	×	×	×	×	×	×	×	✓	×
0	3	0	0	✓	×	×	×	×	✓	×	×	×	×	×
1	3	0	0	×	×	×	×	×	✓	×	×	×	×	×
2	3	0	0	×	×	×	×	×	✓	×	×	×	×	×
3	0	3	0	×	×	×	×	×	×	×	×	×	✓	✓
3	1	3	0	×	×	×	×	×	×	×	×	×	✓	×
3	2	3	0	×	×	×	×	×	×	×	×	×	✓	×
0	3	0	3	✓	×	×	×	×	✓	×	×	×	×	×
1	3	0	3	×	×	×	×	×	✓	×	×	×	×	×
2	3	0	3	×	×	×	×	×	✓	×	×	×	×	×

SELECTION RULES IN THE SUMMATION (13)

(i) One of λ_1 or λ_2 must be 0 or 2.

(ii) Any ΔJ_1, ΔJ_2 is allowed provided one of $|\Delta J_1|$, $|\Delta J_2| \leqslant 2$. $\Delta K_1 = \pm m_1 n_1$, $\Delta K_2 = \pm m_2 n_2$, provided one of m_1, $m_2 = 0$; $m_1 = 0$ if $|\Delta J_2| > 2$, $m_2 = 0$ if $|\Delta J_1| > 2$. Here, m_1 or m_2 is a positive integer or zero, while n_1 or n_2 denotes the rotational symmetry class of molecule 1 or molecule 2 respectively.

Here $n_1 = n_2 = 3$.

(iii) If $K_1 = K_1' = 0$; $K_2 = K_2' = 0$, then $\lambda_1 + \Delta J_1$ and $\lambda_2 + \Delta J_2$ must be even for contribution.

TABLE 4.—GLEBSCH-GORDAN COEFFICIENTS TO BE USED UP TO THE OCTOPOLE TERM IN EQN (13)

(λ_1, λ_2)	no. of times	Clebsch–Gordan coefficients	term
(1, 0) or (0, 1)	2	$C(J, 1, J'; K, 0, K')^2 C(J, 0, J'; K, 0, K')^2$	dipole
(2, 0) or (0, 2)	4	$C(J, 2, J'; K, 0, K')^2 C(J, 0, J'; K, 0, K')^2$	quadrupole
(2, 2)	8	$C(J, 2, J'; K, 0, K')^2 C(J, 2, J'; K, 0, K')^2$	quadrupole
(2, 1) or (1, 2)	10	$C(J, 2, J'; K, 0, K')^2 C(J, 1, J'; K, 0, K')^2$	dipole
(3, 0) or (0, 3)	6	$C(J, 3, J'; K, 0, K')^2 C(J, 0, J'; K, 0, K')^2$	octopole
	2	$C(J, 3, J'; K, 3, K')^2 C(J, 0, J'; K, 0, K')^2$	
(3, 2) or (2, 3)	22	$C(J, 3, J'; K, 0, K')^2 C(J, 2, J'; K, 0, K')^2$	octopole
	6	$C(J, 3, J'; K, 3, K')^2 C(J, 2, J'; K, 0, K')^2$	

The allowed transitions, neglecting multipole terms greater than the octopole, are ticked in table 3, together with the corresponding (λ_1, λ_2) factors allowed by the selection rules, and by general limitations on Clebsch–Gordan coefficients.[24] Summing the different (λ_1, λ_2) factors gives the relevant Clebsch–Gordan coefficients to be used in eqn (13), and these are shown in table 4. For convenience, the summation (13) can be split into the dipole-induced dipole (R^{-6}), quadrupole-induced dipole (R^{-8}) and octopole induced dipole (R^{-10}) terms.

DIPOLE-INDUCED DIPOLE INTENSITY

The intensity of a single dipole-induced ($J \rightarrow J+1$) transition resulting from the bimolecular collision of symmetric top molecules is given from equation (13) and table 4 as:

$$A^{\mu}_{J \rightarrow J+1} = \frac{4\pi^3 \mu^2 N^2}{3hcZ} \int_0^{\infty} 4\pi R^{-4} \exp(-U_{AA}(R)/kT)\, dR \times \sum_{K=-J}^{J} \left[(1 - \exp(-hc\bar{\nu}_1(J)/kT)) \exp(-E_{JK} hc/kT) \bar{\nu}_1(J) \times \left(4\alpha_0^2 f_1(J, K) + \frac{40}{3} \frac{\delta^2 f_1^2(J, K) K^2}{J(J+2)} \right) \right] S(I, K), \quad (14)$$

where $\bar{\nu}_1(J) = 2B(J+1)$, $E_{JK} = BJ(J+1) + (A-B)K^2$ where A and B are the rotational constants,

$$f_1 = (J-K+1)(J+K+1)/(J+1).$$

Thus

$$A^{\mu} = \left(\sum_J A^{\mu}_{J \rightarrow J+1}\right)/N^2. \quad (15)$$

QUADRUPOLE-INDUCED DIPOLE INTENSITY

Similarly, from (13) and table 4:

$$A^{Q}_{J\to J+2} = \frac{4\pi^3 Q^2 N^2}{3hcZ}\int_0^\infty 4\pi R^{-6}\exp(-U_{AA}(R)/kT)\,dR\times \sum_{K=-J}^{J}[(1-\exp(-hc\bar{\nu}_2(J)/kT))\exp(-E_{JK}hc/kT)\bar{\nu}_2(J)\times (18\alpha_0^2 f_2(J,K)+\tfrac{48}{5}\delta^2 f_2^2(J,K))]S(I,K) \quad (16)$$

where $\bar{\nu}_2(J) = 2B(2J+3)$

$$f_2(J,K) = \frac{(J-K+2)(J-K+1)(J+K+2)(J+K+1)}{(J+1)(J+2)(2J+3)}$$

Thus

$$A^{Q} = (\sum_J A^{Q}_{J\to J+2})/N^2. \quad (17)$$

OCTOPOLE-INDUCED DIPOLE INTENSITY

Similarly, from (13) and table 4:

$$A^{\Omega}_{J\to J+3} = \frac{4\pi^3\Omega^2 N^2}{3hcZ}\int_0^\infty 4\pi R^{-8}\exp(-U_{AA}(R)/kT)\,dR\times \sum_{K=-J}^{J}\left[(1-\exp(-hc\bar{\nu}_3(J)/kT))\exp(-E_{JK}hc/kT)\bar{\nu}_3(J)\times \left((24x'+8y)\alpha_0^2+\left(\frac{176x'}{9}+\frac{16y}{3}\right)w\delta^2\right)\right]S(I,K) \quad (18)$$

where

$$x' = \frac{5(J+K+3)(J+K+2)(J+K+1)(J-K+3)(J-K+2)(J-K+1)}{(J+2)(J+3)(2J+2)(2J+3)(2J+5)}$$

$$y = \frac{(J+K+3)(J+K+2)(J+K+1)(J-K+3)(J-K+2)(J-K+1)}{(2J+2)(2J+3)(2J+4)(2J+5)(2J+6)}$$

$$w = \frac{3(J-K+2)(J-K+1)(J+K+1)(J+K+2)}{(2J+2)(2J+3)(J+2)}$$

$$\bar{\nu}_3(J) = 6B(J+2).$$

Thus

$$A^{\Omega} = (\sum_J A^{\Omega}_{J\to J+3})/N^2. \quad (19)$$

THE INTERMOLECULAR POTENTIAL $U_{AA}(R)$

A recent review [25] emphasised that the Lennard-Jones 12–6 potential is an inadequate representation of even inert gas interactions, although it is only in recent years that advances in theoretical and experimental techniques have allowed of the definition of significantly more accurate intermolecular potential energy functions in these simplest cases.

It seems, therefore, that one has the alternatives of:
(*a*) calculating a value of $|Q|$ assuming a tractable functional form for $U_{AA}(R)$; (*b*) determining the integrals in eqn (14), (16) and (18) by numerical integration of a more complicated form of $U_{AA}(R)$ involving, for instance, quadrupole-quadrupole interaction potentials [26] and other non-central modifications to $U_{AA}(R)$.

For simplicity, the first alternative has been chosen, using a Lennard-Jones potential for $U_{AA}(R)$ with the parameters $\varepsilon/\boldsymbol{k}$ and σ obtained by Barnes and Sutton [27] from fitting dielectric and pressure second virial coefficient data. The parameters A^{μ}, A^{Q} and A^{Ω} may also be assessed using Auer's original [28] values of $\varepsilon/\boldsymbol{k}$ and σ. The integrals may then be evaluated using the tables of Buckingham and Pople.[29]

The anisotropy of polarisability factor, $\delta = \alpha_{\parallel} - \alpha_{\perp}$ has been estimated using anisotropic bond polarisabilities [30] in the absence of experimental anisotropy data. The values used are:

$\alpha_0 = 4.58 \times 10^{-24}$ cm^3; $\alpha_{\parallel} = 4.3 \times 10^{-24}$ cm^3; $\alpha_{\perp} = 4.7 \times 10^{-24}$ cm^3. Calculated values of A^{μ}, A^{Q} and A^{Ω} are shown in table 5.

TABLE 5.—THE EFFECT OF VARYING LENNARD-JONES PARAMETERS ON A^{μ}, A^{Q} AND A^{Ω}

σ/nm	εk^{-1}/K	T/K	partition function (Z)	A^{μ}/ cm^{-2}	A^{Q}/ cm^{-2}	A^{Ω}/ cm^{-2}
0.432 [27]	328 [27]	288	274 442	$7.34 \times 10^{-43}\ N^2$	$8.19 \times 10^{9}\ Q^2\ N^2$	$1.38 \times 10^{-43}\ N^2$
0.432 [27]	328 [27]	323	321 421	$6.92 \times 10^{-43}\ N^2$	$7.66 \times 10^{9}\ Q^2\ N^2$	$1.17 \times 10^{-43}\ N^2$
0.492 [28]	286 [28]	288	274 442	$4.63 \times 10^{-43}\ N^2$	$3.94 \times 10^{9}\ Q^2\ N^2$	$0.48 \times 10^{-43}\ N^2$
0.492 [28]	286 [28]	323	321 421	$4.36 \times 10^{-43}\ N^2$	$3.67 \times 10^{9}\ Q^2\ N^2$	$0.43 \times 10^{-43}\ N^2$

* calculated using a value [2] of Ω of 3.3×10^{-50} C m^3.

It can be seen from table 5 that the uncertainty in $U_{AA}(R)$ will be the limiting factor in $|Q|$, followed by the uncertainty in Ω. The values $\sigma = 0.432$ nm, $\varepsilon/\boldsymbol{k} = 328$ K lead to a reasonable agreement between calculated and experimental second dielectric virial coefficients,[27] whereas $\sigma = 0.492$ nm, $\varepsilon/\boldsymbol{k} = 286$ K fail to give even a qualitative account of their virial data. Therefore values of $|Q|$ calculated with the former pair would seem to be the most satisfactory that the 12–6 potential can supply. Defining

$$\Delta = \frac{1}{N}\left(\int_{\text{band}} \alpha(\bar{\nu})\, \mathrm{d}\bar{\nu} - A\right),$$

the data at 323 K and 40.4 bar can be used to estimate a rough value of $|Q|$ using the value of about 3.3×10^{-50} C m^3 for Ω. The coefficients of eqn (8) are listed in table 6 below for this particular set of data, using $\varepsilon/\boldsymbol{k} = 328$ K, $\sigma = 0.432$ nm.

TABLE 6.—CALCULATION OF $|Q|$ FROM LOW AND HIGHER DENSITY DATA

temp./K	pressure/bar	number density/ 10^{21} cm^{-3}	quadrupole/ 10^{40} C m^2
323	40.4	1.46	11
323	67.7	4.46	6
288	liquid	5.28	6

It is found that the octopole-induced dipole intensity is quite important even at molecular number densities as low as 1.5×10^{21} cm^{-3}, where the McClung model demands an average distance travelled between collisions of about 1.5 nm.

The apparent decrease in the calculated moment $|Q|$ at liquid-like densities compared with the corresponding value at the lower gas density is a consequence of the invalidation of the bimolecular model. At the high gaseous and at the liquid

densities, the central molecule is always within range of the rather symmetrically arranged multipole fields of its nearest neighbours. Indeed, the *octopolar* contribution to Δ is the most important at these densities in $CClF_3$, making the estimation of Q uncertain by *as least as much* as the uncertainty in Ω for a chosen value of ε/k and σ.

However, there remains an *indication* from table 6 that $|Q|$ is apparently halved on going from $N = 1.5 \times 10^{21}$ cm^{-3} to 4.46×10^{21} cm^{-3}. This decrease has been observed in carbon dioxide,[19] cyanogen [20] and nitrous oxide.[3] In the first two cases, the quadrupole moment is the major dipole inducing field, since CO_2 and $(CN)_2$ have no octopole, the Q values obtained from the liquid data being 5 times and 2 times less, respectively, than those obtained from the corresponding gaseous data using the bimolecular collision model.

So the present analysis would be most significant for gas data below 40 bar or so, and above 10 bar or so, where the bimolecular collision model would be appropriate. Also, some induced birefringence [32] data on $CClF_3$ might make possible the determination of an accurate quadrupole moment Q, which in turn would enable the determination of a more accurate octopole moment Ω from high precision pressure data over 3–100 cm^{-1} in the range 10–40 bar.

In the meantime, it might be of some interest to compare our rough value of *ca.* 17×10^{-40} C m^2 for $|Q|$ with a value derived from a point charge model with centre of mass coordinates using net charges derived from an extended Hückel molecular orbital theory calculation.[33] This suggests that $|Q|$ is of the order of $3–6 \times 10^{-40}$ C m^2. There is every reason to believe [19, 20, 26] that the value of *ca.* 11×10^{-40} C m^2 given here for $|Q|$ would be about halved if it were recalculated using a non-central potential:

$$U_{AA}(R) + U_{QQ}(R, \theta, \phi)$$

instead of $U_{AA}(R)$, where $U_{QQ}(R, \theta, \phi)$ is the quadrupole-quadrupole interaction potential. However, this exercise would at the same time contradict assumption (1) of the introduction.

The one thing that is quite certain is that for the pseudo-spherical $CClF_3$ molecule, the barrier to rotation even in the closely packed liquid phase, is small enough to allow a process of collision-interrupted free rotation, rather than libration. The far infra-red absorption of the dense gas and liquid is the " collapsed " equivalent of the free rotor line spectrum of the dilute gas phase.

MODEL CALCULATIONS

It has been shown by Davies *et al.*[34] in an earlier paper that it is inappropriate to retain the point multipole model in liquid phase studies. It is preferable to consider the local charges on the individual atoms as producing the field in the near neighbourhood of the molecule. Using a formulation evaluated by Buckingham [35] for the components of radial flux density induced at a point by an axially symmetric charge distribution they were able to compare the field at certain distances from the molecule with that produced by a corresponding point multipole. The two representations were found to be very different at distances close to the inducing molecule. Their calculations were carried out on non-dipolar molecules where only one of the higher moments was assumed to be important. We have repeated this calculation for $CClF_3$ for the first three moments.

For a point P a distance R from the centre of the axially symmetric charge distribution the components of the field are given by

$$F_r = \frac{q}{R^2} + \frac{2\mu\cos\theta}{R^3} + \frac{3Q(3\cos^2\theta - 1)}{2R^4} + \frac{2\Omega(5\cos^3\theta - 3\cos\theta)}{R^5} + \cdots$$

$$F_s = \sin\theta\left[\frac{\mu}{R^3} + \frac{3Q\cos\theta}{R^4} + \frac{3\Omega(5\cos^2\theta - 1)}{2R^5} + \cdots\right] \qquad (20)$$

$$F_t = 0$$

where F_r is the radial component and the components at right angles to R are F_s and F_t, q is the point charge, μ is the point dipole moment, Q is the point quadrupole moment, Ω the point octopole moment and θ is the angle of the radius vector from the point P to the axis of symmetry. For points P at relatively large distances from the centre of symmetry of the molecule along the (C—Cl) bond (about $10l$ and $15l$, where l is the van der Waals radius of the chlorine atom) the field due to both point charges and their point multipole representation would be expected to be in close agreement. Using the following values for the point multipoles: $\mu = 1.7\times10^{-30}$ C m; $Q = 17\times10^{-40}$ C m^2 (this work) and [2] $\Omega = 33\times10^{-50}$ C m^3: The point charges on each of the atoms can be deduced via two simultaneous equations (i.e., at $10l$ and $15l$). Using the charges so obtained and those in the literature the electric field at distances $5l$, $3l$ and l can be found. In a similar manner, using eqn (20), the field due to the point multipoles can be evaluated at the same distances.

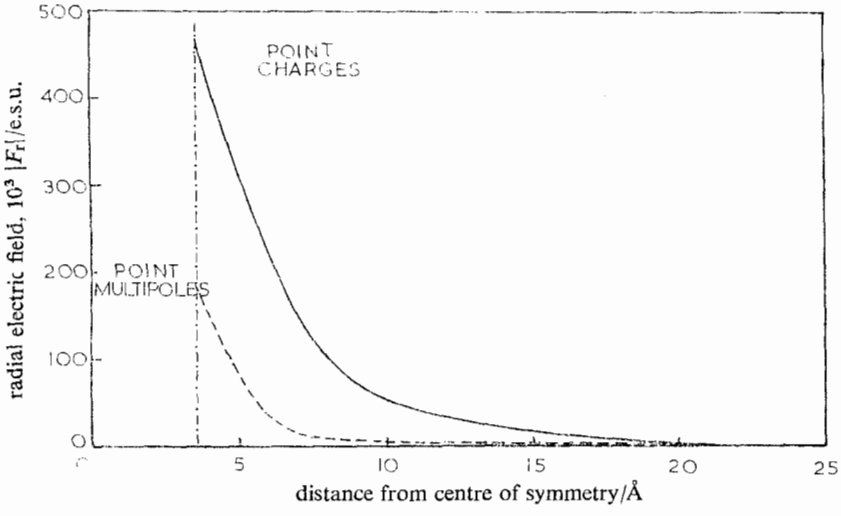

FIG. 9.—Variation of the radial electric field of $CClF_3$ along the (C—Cl) bond for alternative models of representation. —— point charges; - - - - point multipoles; (i.e., point dipole and quadrupole and octupole). The line – · – · – represents the van der Waals radius of the Cl atom.

For $CClF_3$, the charge on each F atom $= 0.26e$; charge on each Cl atom $= 0.10e$; where e = electronic charge. These can be compared with values obtained from m.o. theory [33]: charge on each F atom $= 0.37e$; charge on each Cl atom $= 0.17e$. The agreement of theory and experiment in this evaluation appears to justify the initial assumption of the equivalence of the two representations at large separations of the molecules (i.e., dilute gas densities). The variation of the calculated field at discrete distances from the centre of symmetry of the molecule is shown in fig. 9.

The discrepancy between the two representations is enhanced at distances close to the molecule (i.e., liquid and dense gas phases) and, as the local charge model is thought

to be the better representation of the true situation, then the point multipole representation must be quantitatively seriously in error. This verifies the earlier findings of Davies *et al.* for non-dipolar liquids.

The molecular orbital data lead to an effective permanent dipole value of 1.02 D, compared with 0.88 D from a multipole expansion, from which the first local charges are deduced. These differences are such as to suggest that the first charge model probably approximates to the molecular condition almost as well as present data allow.

APPENDIX 1

For linear molecules, up to the quadrupole term, there are the further restrictions that:

(i) the allowed transitions are any ΔJ_1, ΔJ_2, provided one of ΔJ_1 or ΔJ_2 is 0, or 2.

(ii) $\lambda_1 \geqslant |\Delta J_1|$, $\lambda_1 + |\Delta J_1|$ = even,
$\lambda_2 \geqslant |\Delta J_2|$, $\lambda_2 + |\Delta J_2|$ = even.

(iii) $K_1 = K_2 = 0$.

So the allowed (λ_1, λ_2) are ticked below:

ΔJ_1	ΔJ_2	(0, 1)	(1, 0)	(2, 0)	(0, 2)	(1, 2)	(2, 1)	(2, 2)
1	0	×	✓	×	×	✓	×	×
0	1	✓	×	×	×	×	✓	×
2	1	×	×	×	×	×	✓	×
1	2	×	×	×	×	✓	×	×
2	2	×	×	×	×	×	×	✓
2	0	×	×	✓	×	×	×	✓
0	2	×	×	×	✓	×	×	✓
0	0	translational absorption-important at low frequencies						

DIPOLE-INDUCED DIPOLE ABSORPTION

Using the table above, the full equation for a single $J \rightarrow J+1$ dipole induced dipole transition is given by:

$$
{}_{l}A^{\mu}_{J\rightarrow J+1} = \frac{4\pi^3\mu^2N^2}{3hcZ}\int_0^{\infty} 4\pi R^{-4}\exp(-U_{AA}(R)/kT)\times
$$
$$
(1-\exp(-hc\bar{\nu}_1(J)/kT))\exp(-E_Jhc/kT)\bar{\nu}_1(J)\times
$$
$$
\left[4\alpha_0^2(J+1)+\tfrac{8}{3}\delta^2\frac{(J+1)^2(J+2)}{(2J+3)}\right]
$$

where $\bar{\nu}_1(J) = 2B(J+1)$, $\delta = \alpha_{\parallel}-\alpha_{\perp}$, $E(J) = BJ(J+1)$, Z = rotational partition function.

QUADRUPOLE-INDUCED DIPOLE ABSORPTION

Using the table above, the full equation (including anisotropy of polarisability) for the quadrupole-induced dipolar absorption in a bimolecular encounter of linear molecules is

$$
{}_{l}A^{Q}_{J\rightarrow J+2} = \frac{4\pi^3Q^2N^2}{3hcZ}\int_0^{\infty} 4\pi R^{-6}\exp(-U_{AA}(R)/kT)\,dR\times
$$
$$
(1-\exp(-hc\bar{\nu}_2(J)/kT))\exp(-E_Jhc/kT)\bar{\nu}_2(J)\times
$$
$$
\left[9\alpha_0^2\frac{(J+1)(J+2)}{(2J+3)}+\tfrac{18}{5}\delta^2\left(\frac{(J+1)(J+2)}{(2J+3)}\right)^2\right]
$$

where $\bar{\nu}_2(J) = 2B(2J+3)$.

APPENDIX 2

The Clebsch–Gordan coefficients $C(j_1 3j; m_1 0m)$ and $C(j_1 3j; m_1 3m)$ needed in the octopole-induced term for symmetric tops, were evaluated using the general definition [24]:

$$C(j_1 j_2 j; m_1 m_2 m) = \delta(m, m_1+m_2)\left[\frac{(j_1+j_2-j)!(j+j_1-j_2)!(j+j_2-j_1)!(2j+1)}{(j+j_1+j_2+1)!}\right]^{\frac{1}{2}} \times$$

$$\sum_k \frac{(-1)^k((j_1+m_1)!(j_1-m_1)!(j_2+m_2)!(j_2-m_2)!(j+m)!(j-m)!)^{\frac{1}{2}}}{k!(j_1+j_2-j-k)!(j_1-m_1-k)!(j_2+m_2-k)!(j-j_2+m_1+k)!(j-j_1-m_2+k)!}$$

with $j = j_1+3$, $m_2 = 0, j_2 = 3$; and $j = j_1+3$, $m_2 = 3, j_2 = 3$ respectively. Thus:

$$C(j_1 3j; m_1 0m) = \left[\frac{5(j_1+m+3)(j_1+m+2)(j_1+m+1)(j_1-m+3)(j_1-m+2)(j_1-m+1)}{(j_1+2)(j_1+3)(2j_1+1)(2j_1+2)(2j_1+3)(2j_1+5)}\right]^{\frac{1}{2}}$$

and:

$$C(j_1 3j; m_1 3m) = \left[\frac{(j_1+m+3)(j_1+m+2)(j_1+m+1)(j_1-m+3)(j_1-m+2)(j_1-m+1)}{(2j_1+1)(2j_1+2)(2j_1+3)(2j_1+4)(2j_1+5)(2j_1+6)}\right]^{\frac{1}{2}}.$$

APPENDIX 3

In deriving eqn (8) we have neglected the effects of cross-relaxation between sets of overlapping $J \rightarrow J+n$ lines ($n = 1, 2, 3$), as was pointed out by a referee. The cross relaxation between the permanent and induced dipoles would be the major term not explicitly treated here. However, we feel that this omission is justifiable on the following grounds.

(i) Analogous studies* with the highly dipolar molecules HF, HCl and HBr have established acceptable values of the respective quadrupole moments with complete neglect of overlap relaxation. The dipole of CF_3Cl is much smaller.

(ii) In a preliminary, unpublished study, van Kranendonk (personal communication) has found that assuming isotropic intermolecular forces, hence a spherically symmetric pair distribution function, and further assuming only a "$\mu_1\alpha_2$" effect, a dipole induced dipole, the cross-terms disappear. Cohen (G. Birnbaum, personal communication) is at present engaged in a detailed theoretical study of the whole problem.

(iii) As mentioned earlier, the limiting uncertainty in our values of $|Q|$ comes from that in the Lennard-Jones parameters we have used. That due to cross-relaxation effects is almost certainly negligible in comparison.

Acknowledgement is made to the Director of Research of the Post Office for permission to publish this work. M. W. E. thanks the University College of Wales, Aberystwyth for a Dr. Samuel Williams studentship and the S.R.C. for a post-doctoral fellowship. Prof. Mansel Davies is thanked for reading the manuscript and suggesting several improvements. We also thank Dr. R. E. D. McClung for a copy of the computer program described in ref. (18), and Mr. A. E. Parker of the Post

* S. Weiss and R. H. Cole, *J. Chem. Phys.*, 1967, **46**, 644; W. G. Rothschild, *J. Chem. Phys.*, 1968, **49**, 2250.

Office Research Station for his help in converting the program for use on the S1A, CDC 6600 computer. We also thank Dr. David Parry (U.C.W.) for useful mathematical guidance, and Messrs. John Poley, Bob Meredith and Harold Jolley for essential workshop advice and practice.

[1] B. S. Frost, *J. C. S. Faraday II*, 1973, **69**, 1142.
[2] R. D. Nelson, Jr., and R. H. Cole, *J. Chem. Phys.*, 1971, **54**, 4033.
[3] A. I. Baise, *J. C. S. Faraday II*, 1972, **68**, 1904.
[4] H. A. Gebbie and R. Q. Twiss, *Rep. Progr. Phys.*, 1966, **46**, 396.
[5] A. I. Baise, *Thesis* (University of Wales, 1971); G. J. Davies, *Thesis* (University of Wales, 1971).
[6] J. Chamberlain, *Infra-red Phys.*, 1971, **11**, 25.
[7] J. Chamberlain and H. A. Gebbie, *Infra-red Phys.*, 1971, **11**, 57.
[8] P. E. Clegg and J. S. Huizinga, *I.E.R.E. Conference on Infra-red Techniques*, Reading, England, 1971.
[9] J. Chamberlain, *Infra-red Phys.*, 1971, **12**, 145.
[10] W. Braker and A. L. Mossman, *Matheson Gas Data Book* (Matheson Gas Products, East Rutherford, New Jersey, 5th edn. 1971), p. 149.
[11] J. M. H. Levelt Sengers, J. Straub and M. Vincentini-Missoni, *J. Chem. Phys.*, 1971, **54**, 5034.
[12] A. Michels, T. Wassenaar, G. J. Walkers, Chr. Prins and L. v. d. Klundert, *J. Chem. Eng. Data*, 1966, **11**, 449.
[13] R. M. van Aalst, J. ven der Elsken, D. Frenkel and G. H. Wegdam, *Symp. Faraday Soc.*, 1972, **6**.
[14] R. G. Gordon, *J. Chem. Phys.*, 1965, **43**, 1307.
[15] A. Gerschel, I. Darmon and C. Brot, *Mol. Phys.*, 1972, **23**, 317.
[16] R. E. D. McClung, *J. Chem. Phys.*, 1972, **57**, 5478; *Chem. Phys. Letters*, 1973, **19**, 304.
[17] R. G. Gordon, *J. Chem. Phys.*, 1966, **44**, 1830.
[18] T. E. Eagles and R. E. D. McClung, *Chem. Phys. Letters*, to be published.
[19] G. Birnbaum, W. Ho and A. Rosenburg, *J. Chem. Phys.*, 1971, **55**, 1028.
[20] M. Evans, *J. C. S. Faraday II*, 1973, **69**, 763; *Spectrochim. Acta*, 1974, **30A**, 79.
[21] B. Lassier and C. Brot, *Chem. Phys. Letters*, 1968, **1**, 581; I. W. Larkin, *J. C. S. Faraday II*, 1973, **69**, 1278.
[22] M. Evans, *J. C. S. Faraday II*, 1975, **71**, 71.
[23] R. G. Gordon, *J. Chem. Phys.*, 1963, **38**, 1724.
[24] M. Abramovitz and I. A. Stegun, *Handbook of Mathematical Functions* (Dover, New York, 1965), p. 1006.
[25] G. C. Maitland and E. B. Smith, *Chem. Soc. Rev.*, 1973, **2**, 181.
[26] T. K. Bose and R. H. Cole, *J. Chem. Phys.*, 1970, **62**, 140.
[27] A. N. M. Barnes and L. E. Sutton, *Trans. Faraday Soc.*, 1971, **67**, 2915.
[28] J. O. Hirschfelder, C. F. Curtiss, and R. B. Bird, *Molecular Theory of Gases and Liquids* (Wiley, New York, 1954). p. 1214.
[29] A. D. Buckingham and J. A. Pople, *Trans. Faraday Soc.*, 1955, **51**, 1173.
[30] R. J. W. Le Fèvre, *Adv. Phys. Org. Chem.*, 1965, **3**, 1.
[31] J. P. Colpa and J. A. A. Ketelaar, *Mol. Phys.*, 1958, **1**, 343.
[32] A. D. Buckingham, R. L. Disch and D. A. Dunmur, *J. Amer. Chem. Soc.*, 1968, **90**, 3104.
[33] J. M. Sichel and M. A. Whitehead, *Theor. Chim. Acta*, 1966, **5**, 35.
[34] G. J. Davies, J. Chamberlain and M. Davies, *J. C. S. Faraday II*, 1973, **69**, 1223.
[35] A. D. Buckingham, *Quart. Rev.*, 1959, **13**, 183.

PRINTED IN GREAT BRITAIN AT
THE UNIVERSITY PRESS
ABERDEEN